Transition from antiferromagnetism to superconductivity in the compensated metallic state of $Ba_{1-x}K_x(Fe_{1-y}Co_y)_2As_2$

Shunpei Suzuki,[1] Kenya Ohgushi,[1,2] Yoko Kiuchi,[1] and Yutaka Ueda[1,2]
[1]*Institute for Solid State Physics, University of Tokyo, Kashiwanoha, Kashiwa, Chiba 277-8581, Japan*
[2]*JST, TRIP, Sanbancho, Chiyoda, Tokyo 102-0075, Japan*
(Received 27 August 2010; revised manuscript received 7 October 2010; published 8 November 2010)

We have investigated the electronic properties of $Ba_{1-x}K_x(Fe_{1-y}Co_y)_2As_2$ ($0 \le x \le 0.51, 0 \le y \le 0.22$) single crystals with a special focus on the carrier compensated regions ($x=2y$). With increasing x and y under the $x=2y$ constraint, the ground state changes from an antiferromagnetic metal to a paramagnetic metal with an intervening superconducting phase. On the basis of the Hall coefficient measurements, we show that this transition occurs in a coherent alloy with a Fermi surface similar to $BaFe_2As_2$, and that the antiferromagnetic fluctuations are slightly weakened with increasing degree of alloying. We discuss the role of the randomness introduced by the substitution of Co^{2+} on this transition.

DOI: 10.1103/PhysRevB.82.184510 PACS number(s): 74.25.F−, 72.15.−v, 74.25.Dw

I. INTRODUCTION

There is growing evidence that superconductivity and static antiferromagnetic order compete with each other in Fe-based superconductors (SCs).[1,2] This is in marked contrast with dynamical antiferromagnetic fluctuations which have been theoretically proposed to mediate Cooper pairs with $s_{\pm}$ symmetry.[3,4] The question of how to destabilize the static antiferromagnetic order while retaining the low-energy antiferromagnetic fluctuations is the key to raise the superconducting transition temperature (T_c).

Among the families of Fe-based superconductors, the most well-studied family is the so-called 1-2-2 system with the $ThCr_2Si_2$ structure.[5] The parent compound $BaFe_2As_2$ has hole and electron Fermi surfaces with identical areas, which is a characteristic of a compensated metal.[6] This compound undergoes an antiferromagnetic phase transition at ~140 K, where the crystal structure changes from high-temperature tetragonal $I4/mmm$ into low-temperature orthorhombic $Fmmm$.[7] Although the band nesting is considered to be a key driving factor of the transition, there still remains a controversy over the role of electron correlation effect and the orbital degrees of freedom.[6,8] Superconductivity occurs when the antiferromagnetic order is suppressed and this can be achieved in various ways. One efficient method is by carrier doping, which weakens the nesting condition by enlarging one type of Fermi surface. Hole doping of the Fe sheets through substitution of K^+ ions for Ba^{2+} ions induces superconductivity with T_c as high as 38 K.[9] Electron doping achieved by the substitution of Co^{2+} ions for Fe^{2+} ions also gives rise to superconductivity with $T_c \sim 25$ K.[10,11] Here, it should be underlined that Co^{2+} ions not only modify the Fermi surface[12] but also introduce the carrier scatterers into the system.

Three methods of suppressing the antiferromagnetic order while maintaining the compensated metallic state are available. First, application of hydrostatic pressure to $BaFe_2As_2$ leads to a transition to bulk superconductivity with $T_c = 18$ K at 11 GPa.[13] This is interpreted as preferential lattice shrinking parallel to the crystal layers, leading to a more three-dimensional Fermi surface with weaker nesting character, thus favoring superconductivity. Second, the partial substitution of As atoms with P atoms in $BaFe_2As_2$ induces superconductivity at 31 K.[14,15] Since P substitution renders the Fermi surfaces more three dimensional, this can be regarded as the application of chemical pressure. Third, isovalent substitution of the type $Ba(Fe_{1-y}Ru_y)_2As_2$ leads to superconductivity with a maximum T_c of 20 K.[16] The formation of coherent alloys and the reduced Stoner factor in comparison with $BaFe_2As_2$ due to the extended nature of the Ru $4d$ orbitals have been shown by first-principles calculations.[17] These features have been confirmed by subsequent angle-resolved photoemission spectroscopy.[18]

Singh proposed the possibility of superconductivity in another compensated metal $KFeCoAs_2$.[19] On the basis of band calculations, he pointed out that the Fermi surfaces of $KFeCoAs_2$ resemble those of $BaFe_2As_2$ but have a weaker tendency toward the magnetic order. The resemblance is considered to be much more striking in comparison with $BaFe_2As_2$ substituted by P and Ru atoms with a different chemical trend. Hence, it is not a trivial question to ask whether superconductivity instead of antiferromagnetic order is actually realized in $KFeCoAs_2$. Motivated by this theoretical work, we report on the electronic phase diagram of the solid solution $Ba_{1-x}K_x(Fe_{1-y}Co_y)_2As_2$, as summarized in Fig. 1. This system is unique in the sense that the hole doping by the K^+ substitution and the electron doping by the Co^{2+} substitution are combined. The system thus includes a region where doped holes and electrons are compensated ($x=2y$); the special case is $KFeCoAs_2$ at $x=1$ and $y=1/2$. We demonstrate that the antiferromagnetic metallic phase is destabilized and the superconducting phase appears with increasing degree of alloying on the $x=2y$ line. We then discuss which material parameters trigger this transition.

II. EXPERIMENTAL

Single crystals of $Ba_{1-x}K_x(Fe_{1-y}Co_y)_2As_2$ were synthesized using the flux method. The starting materials Ba, K, FeAs, and CoAs were placed in an alumina crucible. This was then sealed in a double quartz tube under 0.3 atmosphere of Ar. The tube was heated at 1273 K for 2 h, slowly cooled

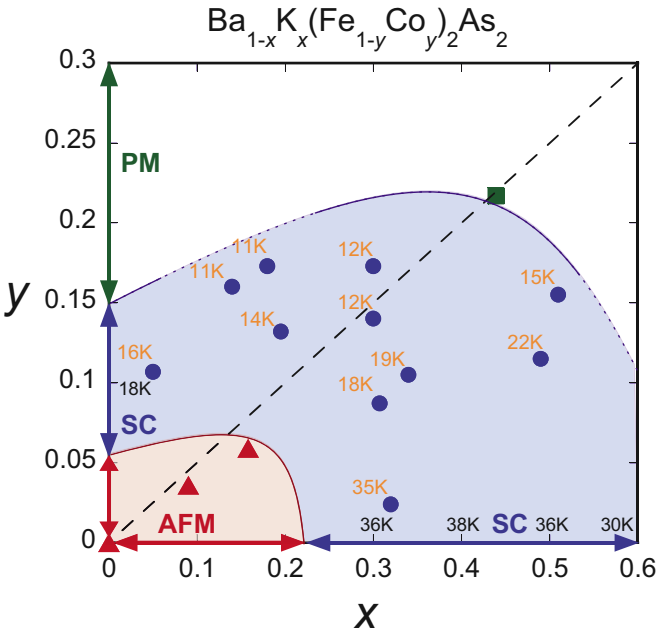

FIG. 1. (Color online) Electronic phase diagram of $Ba_{1-x}K_x(Fe_{1-y}Co_y)_2As_2$ ($0 \le x \le 0.51$ and $0 \le y \le 0.22$) in the x-y plane. Note that the scale of ordinate axis is halved in comparison with that of abscissa axis. The dotted line represents $x=2y$, where the doped holes and electrons are compensated. Closed triangles, closed circles, and closed square represent antiferromagnetic metal (AFM), superconductor (SC), and paramagnetic metal (PM), respectively. Arrowed lines on the abscissa and ordinate axes indicate the composition range for the ground states of $Ba_{1-x}K_xFe_2As_2$ and $Ba(Fe_{1-y}Co_y)_2As_2$ from Refs. 11, 12, and 20 The superconducting transition temperature is also indicated in the figure.

to 1073 K for 24 h, and then quenched to room temperature. The size of the crystal obtained is typically $0.5 \times 0.5 \times 0.1$ mm^3. The chemical composition x and y were determined by an energy-dispersive x-ray spectrometer equipped with a scanning electron microscope. The x-ray diffraction pattern for the powdered crystals at room temperature are well described by the space group $I4/mmm$. The lattice parameter a decreases with increasing x and y, and c increases (decreases) with increasing x (y); these trends are the same as in $Ba_{1-x}K_xFe_2As_2$ and $Ba(Fe_{1-y}Co_y)_2As_2$.[9,21] The magnetic properties were measured using a superconducting quantum interference device magnetometer. The electrical resistivity (ρ) and Hall resistivity (ρ_H) in the a-b plane were measured by using a physical properties measurement system (Quantum Design). When measuring ρ_H, we rotated the sample in the magnetic field of 7 T at a fixed temperature (T). Although the sample thickness could be measured accurately, the error bar for the distance between the voltage electrodes was rather large. Therefore, we do not discuss the absolute value of ρ in this study.

III. RESULTS

Figure 2 shows the T dependence of the in-plane resistivity scaled by the 250 K value $\rho/\rho(250\ \mathrm{K})$ for $Ba_{1-x}K_x(Fe_{1-y}Co_y)_2As_2$. The composition range covers $0 \le x \le 0.51$ and $0 \le y \le 0.22$, and we cannot obtain $KFeCoAs_2$ in a single-crystal form. The data for the hole-rich region ($x > 2y$), the hole-electron compensated region ($x \sim 2y$), and the electron-rich region ($x < 2y$) are separately presented in Figs. 2(a)–2(c), respectively. With decreasing T, the value of ρ of $BaFe_2As_2$ shows a sharp decrease at 136 K, where the magnetic and structural transitions occur simultaneously. Upon substitution, the anomaly in ρ changes to an upturn with an internal structure corresponding to the separated structural transition temperature (T_s) and antiferromagnetic transition temperature (T_N). Following the methodology of earlier reports on $Ba(Fe_{1-y}Co_y)_2As_2$,[1,11] these values are estimated to be $T_s = 131$ K and $T_N = 114$ K for $(x,y) = (0.09, 0.04)$, and $T_s = 107$ K and $T_N = 87$ K for $(x,y) = (0.16, 0.06)$. The value of ρ over a broad composition range

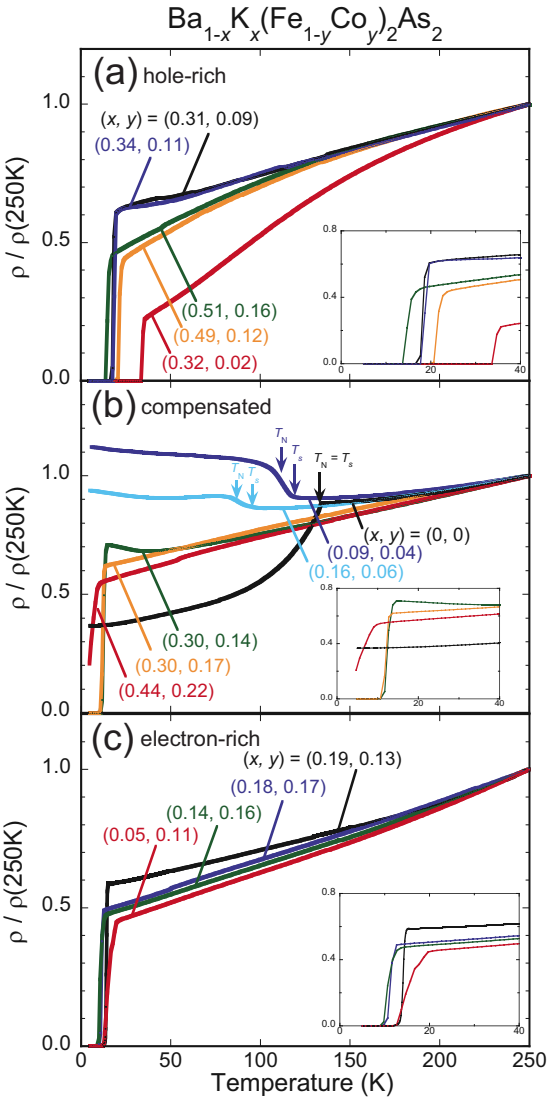

FIG. 2. (Color online) Temperature dependence of the in-plane resistivity scaled by the 250 K value $\rho/\rho(250\ \mathrm{K})$ for $Ba_{1-x}K_x(Fe_{1-y}Co_y)_2As_2$ ($0 \le x \le 0.51$ and $0 \le y \le 0.22$). (a), (b), and (c) cover $x > 2y$, $x \sim 2y$, and $x < 2y$ regions, respectively. The arrows represent the antiferromagentic transition temperature (T_N) and the structural transition temperature (T_s). The insets are the magnified views around the superconducting transition temperature.

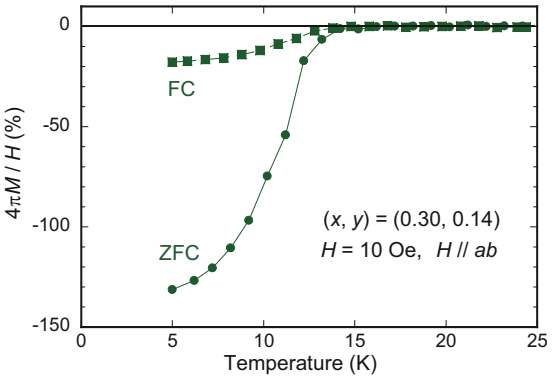

FIG. 3. (Color online) Temperature dependence of the magnetic susceptibility (M/H) under the magnetic field (H) of 10 Oe along the ab plane for $Ba_{1-x}K_x(Fe_{1-y}Co_y)_2As_2$ with $(x,y)=(0.30,0.14)$. FC and ZFC stand for the field-cooled and zero-field-cooled condition, respectively.

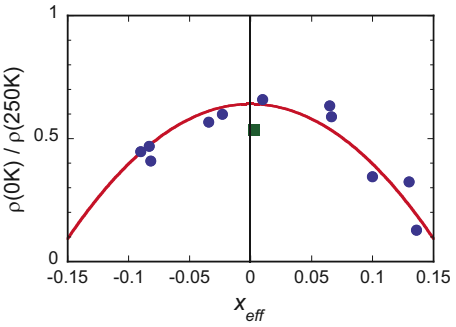

FIG. 4. (Color online) Resistivity ratio $\rho(0\ \mathrm{K})/\rho(250\ \mathrm{K})$ plotted against the effective carrier density $x_{eff}(=x/2-y)$ for $Ba_{1-x}K_x(Fe_{1-y}Co_y)_2As_2$ which ground states are the superconductor (closed circles) or the paramagnetic metal (closed square). The $\rho(0\ \mathrm{K})$ values are extrapolated from the resistivity above the superconducting transition temperature (see text for details). The solid line is a guide for the eye.

drops to zero at low T, indicating the onset of superconductivity. This superconductivity is a bulk property, as evidenced by the Messiner signal shown in Fig. 3. The volume fraction exceeds 100%; this originates from experimental errors in measuring the mass of a small single crystal. T_c is estimated from the midpoint of the resistivity drop, and the transition width is typically 2 K. At $(x,y)=(0.44,0.22)$, ρ shows a decrease below $\sim$10 K but does not reach zero. We conclude that the superconductivity is filamentary and the bulk material is in the paramagnetic state. The ground-state properties obtained as above, as well as those reported for $Ba_{1-x}K_xFe_2As_2$ and $Ba(Fe_{1-y}Co_y)_2As_2$ are summarized as an electronic phase diagram in Fig. 1.

ρ in the paramagnetic state exhibits characteristic T variations depending on the type of the dominant carrier. For hole dominant compositions [Fig. 2(a)], ρ shows a strong upward-concave T dependence over a wide T range, being reminiscent of the Bloch-Grüneisen formula caused by phonon scattering. At $(x,y)=(0.32,0.02)$, (0.31, 0.09), and (0.34, 0.11), the upward-concave behavior is taken over by the downward-concave one below 80–90 K whereas it persists down to T_c in $(x,y)=(0.49,0.12)$, and (0.51, 0.16). On the other hand, ρ in the electron dominant composition range [Fig. 2(c)] shows a downward-concave T dependence over the whole T range measured, as is frequently observed in the correlated electron systems. It should be noted that this feature is also seen in the other electron doped 1-2-2 compounds $Ba(Fe_{1-y}M_y)_2As_2$ (M=Co, Ni, Rh, Pd, and Pt).[22–25] This type of particle-hole asymmetric charge dynamics has been discussed in an earlier study of $Ba(Fe_{1-x}Ru_x)_2As_2$, in which the resistivity of the hole and electron bands (ρ_h and ρ_e) were shown to display upward- and downward-concave T dependence, respectively.[16] Our results are in harmony with this conclusion: ρ is written as $\rho=1/(\sigma_h+\sigma_e)$ with $\sigma_h=1/\rho_h$ and $\sigma_e=1/\rho_e$ in the two carrier model, and the σ_h- and σ_e-term becomes dominant in the hole- and electron-rich composition regions, respectively. However, the microscopic mechanism of the distinct T dependence between ρ_h and ρ_e is still unclear.

Figure 4 plots $\rho(0\ \mathrm{K})/\rho(250\ \mathrm{K})$ against the effective carrier density $x_{eff}(=x/2-y)$, where $\rho(0\ \mathrm{K})$ is deduced by fitting ρ between 80 K and T_c with the function $\rho=\rho(0\ \mathrm{K})+AT^n$ (A and n being the fitting parameters). $\rho(0\ \mathrm{K})/\rho(250\ \mathrm{K})$ clearly shows a maximum at $x_{eff}=0$. This conflicts the conclusion of the two independent carrier model with the rigid band approximation,[23] where $\rho(x_{eff},0\ \mathrm{K})/\rho(x_{eff},250\ \mathrm{K})\sim\rho(0,0\ \mathrm{K})/\rho(0,250\ \mathrm{K})$ $(1+A'x_{eff})+O(x_{eff}^2)$ (A' being a constant value) indicates the linear x_{eff} dependence of $\rho(0\ \mathrm{K})/\rho(250\ \mathrm{K})$ in the low x_{eff} range. One plausible reason of this discrepancy is that the interaction between hole and electron bands in a nearly perfect nesting condition gives rise to a poor metallic charge dynamics characterized by a large $\rho(0\ \mathrm{K})/\rho(250\ \mathrm{K})$ value at $x_{eff}=0$.

A peculiar feature of the phase diagram shown in Fig. 1 is that the superconducting phase exists in $x\sim2y$. This is in stark contrast to the naive expectation that the antiferromagnetic state is realized owing to the band nesting. Moreover, the paramagnetic state is stabilized at $(x,y)=(0.44,0.22)$. Hence, the ground state changes from antiferromagnetic metal (AFM) to paramagnetic metal (PM) with an intervening superconductor with increasing x and y on the $x=2y$ line.

In order to gain further information on this phase transition, we performed Hall coefficient (R_H) measurements for the six $x\sim2y$ samples. According to the previous analysis for $Ba_{1-x}K_xFe_2As_2$ and $Ba(Fe_{1-y}Co_y)_2As_2$, the sign and magnitude of R_H in the normal state is sensitive to the excess carrier density from the compensated metallic state.[23,26,27] Typically, R_H with the positive (negative) value increases in magnitude with decreasing T in the hole- (electron-) rich compositions. As can be seen from Fig. 5, the values of R_H at 250 K are comparable among these six samples, indicating that the carrier density (Fermi-surface area) of the $x\sim2y$ compounds actually remains quite similar to that of $BaFe_2As_2$. In other words, the Co^{2+} substitution leads to the formation of a coherent alloy with an upward Fermi-energy shift corresponding to the y value, and the doped electrons are fully compensated by the $x/2$ holes introduced by the K^+ substitution.

At $(x,y)=(0,0)$, (0.09, 0.04), and (0.16, 0.06), R_H shows discontinuous jumps at 140 K, 110 K, and 90 K, respectively,

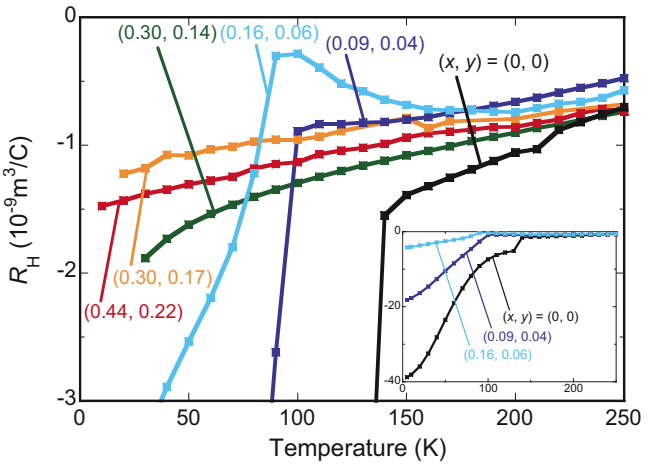

FIG. 5. (Color online) Temperature dependence of the Hall coefficient R_H for $Ba_{1-x}K_x(Fe_{1-y}Co_y)_2As_2$ with the carrier compensated compositions ($x \sim 2y$). The inset shows the same data in a wider scale.

in excellent agreement with the values of T_N estimated from ρ. In the paramagnetic state, R_H gradually increases in magnitude with decreasing T except at $(x,y)=(0.16,0.06)$; this T variation originates from the antiferromagnetic fluctuations.[15,23] With departure from $x=y=0$, the T variation becomes slightly weaker, inferring that the antiferromagnetic fluctuations are weakened even in the similar Fermi surfaces of $BaFe_2As_2$. The reason why R_H for $(x,y)=(0.16,0.06)$ shows a nonmonotonic T dependence is probably due to the deviation of the composition from the $x=2y$ line.

IV. DISCUSSION

We now discuss the mechanism of the antiferromagnetic metal-superconductor transition on the $x=2y$ line. The reduction in antiferromagnetic fluctuations in the paramagnetic state and subsequent destabilization of antiferromagnetic order upon K^+ and Co^{2+} substitution is qualitatively consistent with the results of the first-principles calculations for $KFeCoAs_2$.[19] In the theory, the reason for the weaker magnetic instability is attributed to the reduction in the density of states (Stoner factor) due to the shorter a. The lattice parameters for the parent compound ($x=y=0$) and the superconducting sample with $(x,y)=(0.30,0.14)$ are $a=3.952$ Å and $c=13.01$ Å, and $a=3.913$ Å and $c=13.12$ Å, respectively. It is not clear whether this small in-plane contraction ($\sim 1.0\%$) gives rise to the reduction in the density of states which is enough to destabilize the static magnetic order. In this case, we notice that the pressure effect hardly explains the appearance of superconductivity since lattice shrinkage is $\sim 1.0\%$, being much smaller than $\sim 10\%$ shrinkage of $BaFe_2As_2$ under a pressure of 11 GPa.[28]

Besides the chemical pressure effect, we need to seriously consider the randomness in the alloys.[17] The antiferromagnetic alignment due to the band nesting is supposed to be destroyed by the disorder effect since it generally smoothens the singular structure of the band dispersion. Moreover, it is clarified that an orbital polarized Fermi surface is formed following the concomitant magnetic and structural transition in $BaFe_2As_2$;[6] the addition of Co^{2+} ions with one excess electron among the $3d$ manifold likely destabilizes the spin/orbital ordered state. Hence, it is probable that the site disorder introduced by the Co^{2+} substitution is the key parameter in the antiferromagnetic metal-superconductor transition. It is unclear which of the two mechanisms—the lattice parameter change and the disorder effect—is actually more responsible. Nevertheless, we propose that the introduction of randomness is the effective phase control method for situations when superconductivity and antiferromagnetism are competing in a bicritical manner.[29] In order to establish this conclusion, further experiments are expected to be performed in the future.

We next discuss how the superconducting phase is overtaken by the paramagnetic metallic phase at $(x,y)=(0.44,0.22)$. At this composition, R_H still shows a T variation, indicative of the presence of antiferromagnetic fluctuations. This is in stark contrast to $Ba(Fe_{1-y}Co_y)_2As_2$, where the antiferromagentic fluctuations are largely smeared out when the superconductivity disappears.[30,31] This contrasting behavior is likely to be related to the differences in the Fermi surface. In $Ba(Fe_{1-y}Co_y)_2As_2$, most of the hole Fermi surfaces disappear in the vicinity of the superconductor-paramagnetic metal transition[12] whereas there are hole and electron Fermi surfaces with a nesting character in $Ba_{1-x}K_x(Fe_{1-y}Co_y)_2As_2$ with $x=2y$. Hence, we speculate that the superconductivity is not destroyed by the weakened antiferromagentic fluctuations as a glue of Cooper pairs in the present system. A more plausible scenario is a pair-breaking effect due to the Co^{2+} ions,[32] which enter into the conducting Fe sheets. From our results, we estimate the critical Co^{2+} concentration to be $y_c=0.17-0.22$.[33] This value is much smaller than the percolation threshold of impurities on the nearest-neighbor square lattice model 0.41.[19,34] The pair breaking effect induced by the disorder is also relevant to the T_c decrease. Indeed, as can be seen from Fig. 1, T_c has a tendency to decrease with increasing y. Since various factors relevant to T_c such as the lattice constant (pnictogen height) and Fermi-surface shape also varies in the x-y plane, quantitative arguments on T_c are fairly difficult.

V. CONCLUSIONS

We report on the resistivity and Hall coefficient for single crystal $Ba_{1-x}K_x(Fe_{1-y}Co_y)_2As_2$ $(0 \le x \le 0.51, 0 \le y \le 0.22)$. We found a transition from the antiferromagnetic to paramagnetic phase via a superconducting phase on the $x=2y$ line. The static antiferromagnetic order is destabilized by the combined effect of the in-plane lattice contraction and the site disorder introduced by the Co^{2+} substitution. The superconducting phase is replaced by a paramagnetic phase owing to the pair-breaking effect of the substituted Co^{2+} ions.

ACKNOWLEDGMENTS

The authors are grateful to K. Kuroki, M. Isobe, H. Ueda, T. Yamauchi, T. Kuwabara, and H. Yamauchi for valuable discussions. This work was partly supported by Special

Coordination Funds for Promoting Science and Technology, Promotion of Environmental Improvement for Independence of Young Researchers from the Ministry of Education, Culture, Sports, Science and Technology of Japan.

[1] D. K. Pratt, W. Tian, A. Kreyssig, J. L. Zarestky, S. Nandi, N. Ni, S. L. Bud'ko, P. C. Canfield, A. I. Goldman, and R. J. McQueeney, Phys. Rev. Lett. **103**, 087001 (2009).
[2] J. T. Park, D. S. Inosov, Ch. Niedermayer, G. L. Sun, D. Haug, N. B. Christensen, R. Dinnebier, A. V. Boris, A. J. Drew, L. Schulz, T. Shapoval, U. Wolff, V. Neu, X. Yang, C. T. Lin, B. Keimer, and V. Hinkov, Phys. Rev. Lett. **102**, 117006 (2009).
[3] I. I. Mazin, D. J. Singh, M. D. Johannes, and M. H. Du, Phys. Rev. Lett. **101**, 057003 (2008).
[4] K. Kuroki, S. Onari, R. Arita, H. Usui, Y. Tanaka, H. Kontani, and H. Aoki, Phys. Rev. Lett. **101**, 087004 (2008).
[5] J. Leciejewicz, S. Siek, and A. Szytula, J. Less-Common Met. **144**, L9 (1988).
[6] T. Shimojima, K. Ishizaka, Y. Ishida, N. Katayama, K. Ohgushi, T. Kiss, M. Okawa, T. Togashi, X.-Y. Wang, C.-T. Chen, S. Watanabe, R. Kadota, T. Oguchi, A. Chainani, and S. Shin, Phys. Rev. Lett. **104**, 057002 (2010).
[7] M. Rotter, M. Tegel, D. Johrendt, I. Schellenberg, W. Hermes, and R. Pöttgen, Phys. Rev. B **78**, 020503 (2008).
[8] M. D. Johannes and I. I. Mazin, Phys. Rev. B **79**, 220510(R) (2009).
[9] M. Rotter, M. Tegel, and D. Johrendt, Phys. Rev. Lett. **101**, 107006 (2008).
[10] A. S. Sefat, R. Jin, M. A. McGuire, B. C. Sales, D. J. Singh, and D. Mandrus, Phys. Rev. Lett. **101**, 117004 (2008).
[11] J.-H. Chu, J. G. Analytis, C. Kucharczyk, and I. R. Fisher, Phys. Rev. B **79**, 014506 (2009).
[12] V. Brouet, M. Marsi, B. Mansart, A. Nicolaou, A. Taleb-Ibrahimi, P. Le Fèvre, F. Bertran, F. Rullier-Albenque, A. Forget, and D. Colson, Phys. Rev. B **80**, 165115 (2009).
[13] T. Yamazaki, N. Takeshita, R. Kobayashi, H. Fukazawa, Y. Kohori, K. Kihou, C.-H. Lee, H. Kito, A. Iyo, and H. Eisaki, Phys. Rev. B **81**, 224511 (2010).
[14] S. Jiang, H. Xing, G. Xuan, C. Wang, Z. Ren, C. Feng, J. Dai, Z. Xu, and G. Cao, J. Phys.: Condens. Matter **21**, 382203 (2009).
[15] S. Kasahara, T. Shibauchi, K. Hashimoto, K. Ikada, S. Tonegawa, R. Okazaki, H. Shishido, H. Ikeda, H. Takeya, K. Hirata, T. Terashima, and Y. Matsuda, Phys. Rev. B **81**, 184519 (2010).
[16] F. Rullier-Albenque, D. Colson, A. Forget, P. Thuéry, and S. Poissonnet, Phys. Rev. B **81**, 224503 (2010).
[17] L. Zhang and D. J. Singh, Phys. Rev. B **79**, 174530 (2009).
[18] V. Brouet, F. Rullier-Albenque, M. Marsi, B. Mansart, M. Aichhorn, S. Biermann, J. Faure, L. Perfetti, A. Taleb-Ibrahimi, P. Le Fèvre, F. Bertran, A. Forget, and D. Colson, Phys. Rev. Lett. **105**, 087001 (2010).
[19] D. J. Singh, Phys. Rev. B **79**, 174520 (2009).
[20] M. Rotter, M. Pangerl, M. Tegel, and D. Johrendt, Angew. Chem., Int. Ed. **47**, 7949 (2008).
[21] N. Ni, M. E. Tillman, J.-Q. Yan, A. Kracher, S. T. Hannahs, S. L. Bud'ko, and P. C. Canfield, Phys. Rev. B **78**, 214515 (2008).
[22] L. J. Li, Y. K. Luo, Q. B. Wang, H. Chen, Z. Ren, Q. Tao, Y. K. Li, X. Lin, M. He, Z. W. Zhu, G. H. Cao, and Z. A. Xu, New J. Phys. **11**, 025008 (2009).
[23] N. Katayama, Y. Kiuchi, Y. Matsushita, and K. Ohgushi, J. Phys. Soc. Jpn. **78**, 123702 (2009).
[24] N. Ni, A. Thaler, A. Kracher, J. Q. Yan, S. L. Bud'ko, and P. C. Canfield, Phys. Rev. B **80**, 024511 (2009).
[25] S. R. Saha, T. Drye, K. Kirshenbaum, N. P. Butch, P. Y. Zavalij, and J. Paglione, J. Phys.: Condens. Matter **22**, 072204 (2010).
[26] F. Rullier-Albenque, D. Colson, A. Forget, and H. Alloul, Phys. Rev. Lett. **103**, 057001 (2009).
[27] L. Fang, H. Luo, P. Cheng, Z. Wang, Y. Jia, G. Mu, B. Shen, I. I. Mazin, L. Shan, C. Ren, and H.-H. Wen, Phys. Rev. B **80**, 140508(R) (2009).
[28] J.-E. Jørgensen, J. Staun Olsen, and L. Gerward, Solid State Commun. **149**, 1161 (2009).
[29] Even in the nonisovalent substituted system such as $Ba(Fe_{1-y}Co_y)_2As_2$, we speculate that not only the carrier doping but also the randomness play a role in suppressing the antiferromagnetic order.
[30] F. L. Ning, K. Ahilan, T. Imai, A. S. Sefat, M. A. McGuire, B. C. Sales, D. Mandrus, P. Cheng, B. Shen, and H.-H. Wen, Phys. Rev. Lett. **104**, 037001 (2010).
[31] K. Matan, S. Ibuka, R. Morinaga, S. Chi, J. W. Lynn, A. D. Christianson, M. D. Lumsden, and T. J. Sato, Phys. Rev. B **82**, 054515 (2010).
[32] S. Onari and H. Kontani, Phys. Rev. Lett. **103**, 177001 (2009).
[33] This critical Co^{2+} concentration is larger than that in $Ba(Fe_{1-y}Co_y)_2As_2$, $y_c \sim 0.15$; this supports the different origin of the superconductor-paramagnetic metal transition between the two systems.
[34] M. J. Lee, Phys. Rev. E **78**, 031131 (2008).